Chemical Geology 401 (2015) 15–27

Contents lists available at ScienceDirect

Chemical Geology

journal homepage: www.elsevier.com/locate/chemgeo

Chemical fluxes from time series sampling of the Irrawaddy and Salween Rivers, Myanmar

Hazel Chapman [a,*], Mike Bickle [a], San Hla Thaw [b], Hrin Nei Thiam [b]

[a] Earth Sciences, University of Cambridge, Downing St., Cambridge CB2 3EQ, UK
[b] Department of Meteorology & Hydrology, 50 Kaba-Aye Pogoda Rd, Mayangon 11061, Yangon, Myanmar

ARTICLE INFO

Article history:
Received 2 September 2014
Received in revised form 6 February 2015
Accepted 9 February 2015
Available online 19 February 2015

Editor: David R. Hilton

Keywords:
Irrawaddy
Salween
River chemistry
Myanmar (Burma)
Sr-isotopes
Himalayas

ABSTRACT

The Irrawaddy and Salween rivers in Myanmar deliver water fluxes to the ocean equal to ~70% of the Ganges–Brahmaputra river system. Together these systems are thought to deliver about half the dissolved load from the tectonically active Himalayan–Tibetan orogen. Previously very little data was available on the dissolved load and isotopic compositions of these major rivers. Here we present time series data of 171 samples collected fortnightly at intervals throughout 2004 to 2007 from the Irrawaddy and Salween at locations near both the river mouths, the up-stream Irrawaddy at Myitkyina, the Chindwin, a major tributary of the Irrawaddy and a set of 28 small tributaries which rise in the flood plain of the Irrawaddy between Yangon and Mandalay. The samples have been analysed for major cation, anion and $^{87}Sr/^{86}Sr$ ratios. The new data indicates that the Irrawaddy has an annual average Na concentration only a third of the widely quoted single previously published analysis. The Irrawaddy and Salween drain about 0.5% of global continental area and deliver about 3.3% of the global silicate-derived dissolved Ca + Mg fluxes and 2.6% of the global Sr riverine fluxes to the oceans. This compares with Ganges and Brahmaputra which deliver about 3.4% of the global silicate-derived dissolved Ca + Mg fluxes and 3.2% of the global Sr riverine fluxes to the oceans from about 1.1% of global continental area. The discharge-weighted mean $^{87}Sr/^{86}Sr$ ratio of the Irrawaddy is 0.71024 and the Salween 0.71466.

The chemistry of the Salween and the Irrawaddy waters reflects their different bedrock geology. The catchment of the Salween extends across the Shan Plateau in Myanmar through the Eastern syntaxis of the Himalayas and into Tibet. The Irrawaddy flows over the Cretaceous and Tertiary magmatic and metamorphic rocks exposed along the western margin of the Shan Plateau and the Cretaceous to Neogene Indo-Burma ranges. The $^{87}Sr/^{86}Sr$ compositions of the Salween and Upper Irrawaddy (between 0.7128 and 0.7176) are significantly higher than the downstream Irrawaddy (0.7095 to 0.7108) and the Chindwin (0.7082 to 0.7095). The Irrawaddy and the Chindwin exhibit lower $^{87}Sr/^{86}Sr$ and Na/Ca ratios during and immediately post-monsoon, interpreted to reflect higher weathering of carbonate at high flow. The Salween exhibits higher $^{87}Sr/^{86}Sr$ ratios but lower Na/Ca ratios during the monsoon, interpreted to reflect higher inputs from the upper parts of the catchment in the Himalayas.

1. Introduction

The Himalaya–Tibet region covers just less than 5% of global continental area but the orogen is drained by ten major rivers which supply ~10% of the riverine discharge to the oceans (Fig. 1). The network of rivers includes the Ganges and Brahmaputra in India and Bangladesh, the Irrawaddy and Salween flowing into the Andaman Sea from Myanmar, the Indus from Pakistan and the Chang Jiang (Yangtze), Huang Ho, Zhujiang (Pearl), the Hong (Red) and the Mekong rivers which flow across Tibet, China, or Vietnam. These major rivers carry a significant fraction of the global chemical weathering flux to the oceans (e.g. Palmer and Edmond, 1989; Sarin et al., 1989; Edmond, 1992; Harris et al., 1998; Krishnaswami and Singh, 1998; Singh and Hasnain, 1998; Galy and France-Lanord, 1999; Pandey et al., 1999; English et al., 2000; Bickle et al., 2001; West et al., 2002; Bickle et al., 2003; Bickle et al., 2005; Tipper et al., 2006).

Studies of the physical and chemical weathering caused by these rivers provide a measure of the overall impact of the Himalaya–Tibetan orogen on global climate. A controversial postulate is that exhumation and erosion of the Himalaya–Tibet orogen have increased the 'weatherability' of the continental crust and contributed to the late Cenozoic cooling of global climate and impacted key oceanic tracers such as $^{87}Sr/^{86}Sr$ ratios (Raymo et al., 1988; Raymo and Ruddiman, 1992; Richter et al., 1992; Caldeira et al., 1993; Bickle, 1996).

This study reports chemical and strontium isotope fluxes from the Irrawaddy, Chindwin and Salween Rivers in Myanmar, by analysis of samples collected over a period between 2004 and 2007 at four sites,

* Corresponding author. Tel.: +44 1223 333400.
E-mail address: hjc1000@cam.ac.uk (H. Chapman).

http://dx.doi.org/10.1016/j.chemgeo.2015.02.012
0009-2541/

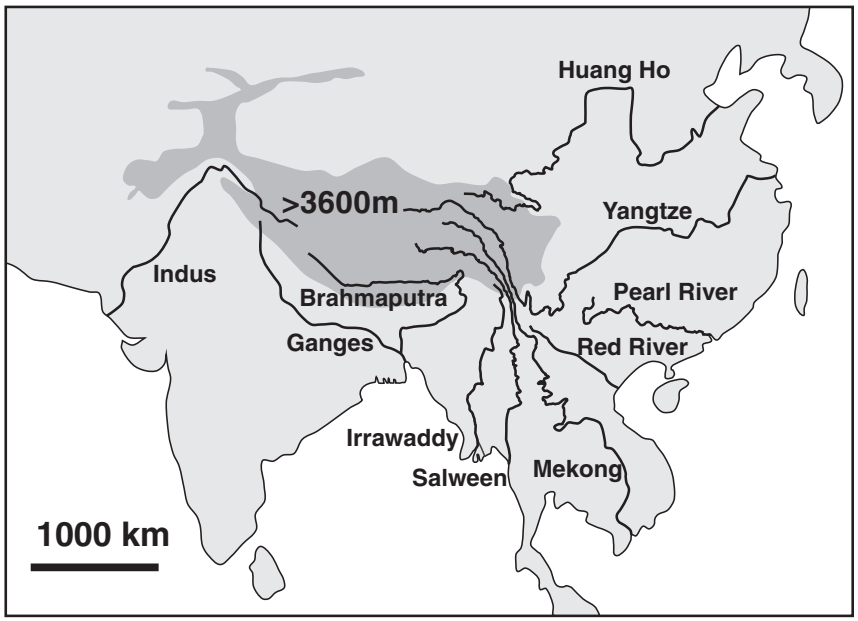

Fig. 1. Major rivers draining the Himalayan–Tibetan region in Asia. Redrawn after Bickle (1996) and Clark et al. (2004).

as well as a set of twenty eight tributaries to the Irrawaddy collected during the 2007 monsoon (Fig. 2). The objective is to determine the chemical and Sr-isotopic fluxes and the controls on these fluxes. These rivers drain an area close to half the size of the catchment area of the Ganges–Brahmaputra system but contribute about 70% of the discharge of the Ganges–Brahmaputra system. Very limited chemical data and no Sr-isotopic data have previously been published for the Irrawaddy and Salween Rivers (e.g. Meybeck and Ragu, 1996).

2. Study area

The Salween rises in Tibet, flows through the Eastern syntaxis of the Himalayas and then flows through China and eastern Myanmar before reaching the Gulf of Martaban (Fig. 1). The Irrawaddy rises in northern Myanmar, and is joined by a major tributary, the Chindwin, just west of Mandalay before reaching the Andaman Sea south of Yangon. The Irrawaddy (Ayeyarwady) River is ranked as having the fifth largest suspended load at 364 +/− 60 MT and the fourth highest total dissolved load of the world's rivers (Robinson et al., 2007). However given the reduced sediment load due to the effects of dams in the Yangtze and Mekong Rivers, it is probable that the Irrawaddy now delivers the third highest sediment load to the ocean after the Amazon and Ganges–Brahmaputra (Robinson et al., 2007). Milliman and Meade (1983) estimate that close to 20% of the current ocean input of water, sediment and dissolved load from the Himalayas and Tibet is delivered by the Irrawaddy–Salween river system.

The Irrawaddy River is 1985 km long and drains a catchment of 413,000 km^2 (Robinson et al., 2007). It is named from the confluence of the N'mai and Mali Rivers in Kachin State. Both the N'mai and Mali Rivers have glacial sources in the vicinity of 28° N in Northern Myanmar. The upstream water samples for this study were collected at a site in the upper reaches of the Irrawaddy at Myitkyina which lies ~50 km south of the confluence (Fig. 2). In 2008, after the sampling for this study was complete, construction work started for the Myitsone Dam at the confluence of the N'mai and Mali Rivers.

Between Myitkyina and Mandalay, the Irrawaddy flows through the Bhamo alluvial basin over the Tagaung-Myklyna Belt to the Mogok Metamorphic Belt. At Mogok, about 100 km north of Mandalay, the river flows almost due south over metamorphic rocks and Holocene lavas. From Mandalay the river makes an abrupt turn westwards, crosses the Sagaing Fault onto the western sedimentary basin, before curving southwest to unite with the Chindwin River, after which it continues in a southerly direction. The Irrawaddy is thought to have drained the Yarlung-Tsang Po in Tibet from at least 40 Ma before capture of the Yarlung-Tsang Po by the Brahmaputra, most probably at ~20 Ma in the early Miocene (Robinson et al., 2013). It is also probable that the upper Irrawaddy originally flowed south from Mandalay, discharging its water through the present Sittoung River to the Gulf of Martaban, and that its present westward course is geologically recent. The delta of the Irrawaddy begins about 93 km above Hinthada (Henzada) and about 290 km from its discharge into the Andaman Sea. The downstream time series was collected close to Hinthada (Fig. 2).

The Chindwin originates in the broad Hukawng Valley of Kachin State where 4 rivers meet. The Tanai exits the Hukawng valley through the Taron or Turong valley and then takes on the name of Chindwin, and maintains a general southerly course. It then takes a more southeasterly course entering into broad central plain, passing the city of Monywa where the time series for the Chindwin were collected. It enters the Irrawaddy just south of Monywa at 21° 27′N 95°17′E. The Chindwin is 1046 km long and has a catchment area of 115,300 km^2 and the discharge in 2004 was ~165 km^3/yr (data from Department of Meteorology & Hydrology, Myanmar) but in severe flood years is ~300 km^3/yr (Zin et al., 2009).

Twenty eight tributaries, which flow west across the lower flood plain between Yangon and Mandalay, were sampled by the first two authors in September 2007 during the monsoon (Fig. 2) in order to investigate the chemical inputs to the Lower Irrawaddy from the younger source rocks in this low altitude catchment area.

The Salween (Thanlwin) River is approximately 2800 km in length, drains a catchment of 2.72×10^5 km^2 and has an average annual discharge of 211 km^3 (Robinson et al., 2007). It rises with water from glaciers in the Tangula Mountains of the Tibetan Plateau, flowing southwards through Yunnan Province of China, the Kayan and Mon States of Myanmar into the Gulf of Martaban in the Andaman Sea. The time-series sample site was at Hpa-An before the outflow into the Gulf of Martaban (Fig. 2).

3. Geology

There are three distinct geological provinces in central Myanmar. Mitchell (1993) describes the geology in detail in terms of the Indian Plate, Burma Plate and Asian Plate. Fig. 3, redrawn from Mitchell et al.

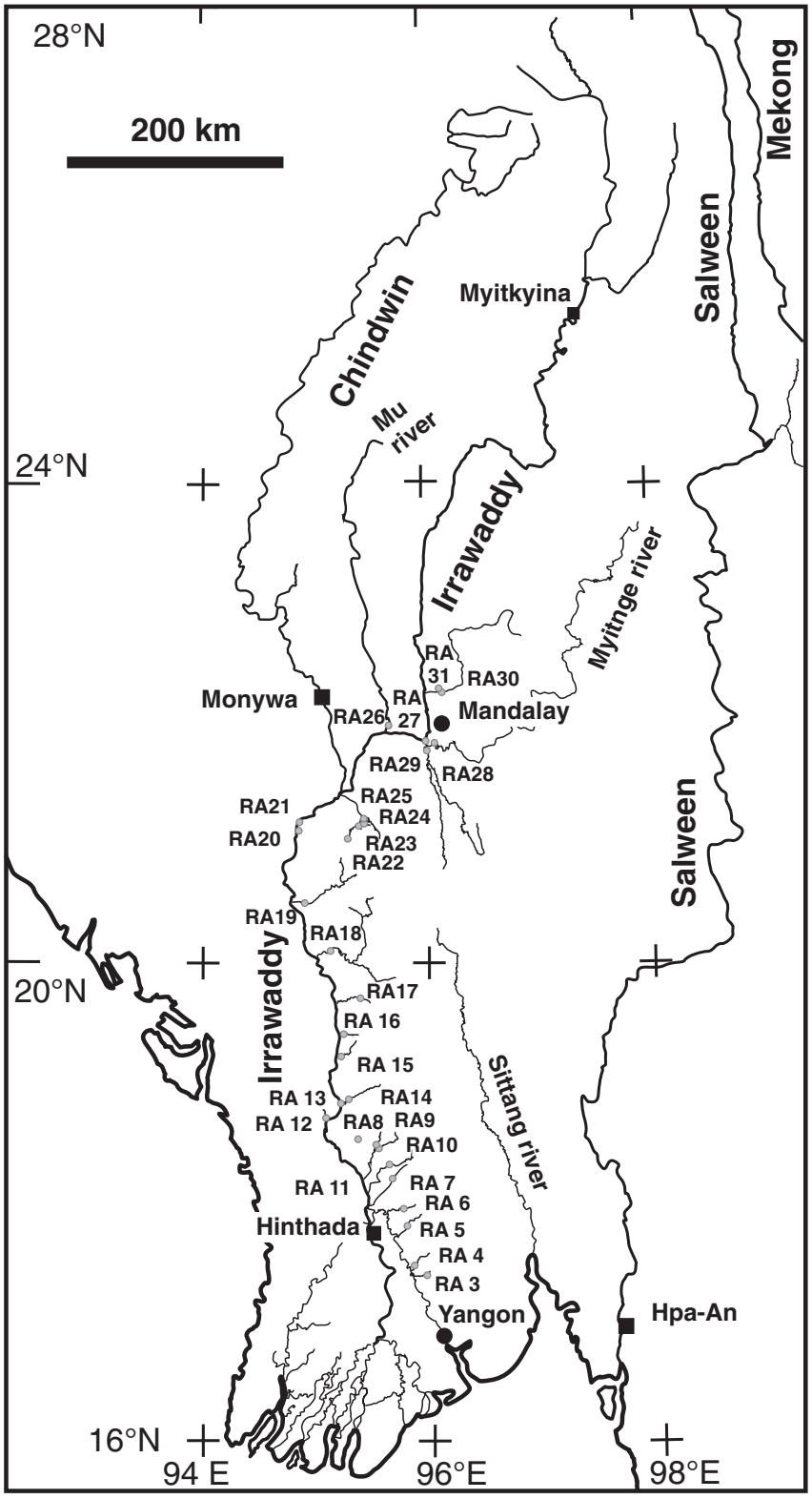

Fig. 2. Map of rivers in Myanmar and sample sites. Drawn from Army Map Service (GDVLB) (1955) 1:250,000 sheets. Solid squares denote the four time-series sample sites. Small grey circles denote tributaries sampled in summer 2007.

(2007) and Searle et al. (2007), illustrates the distribution and ages of the main rock-types.

In the East, the generally older Palaeozoic sediments of the Asian Plate form the highlands of the Shan Plateau incorporating Lower Palaeozoic turbidites and Permian to Triassic carbonates. The western boundary of this zone is the Mogok Metamorphic Belt, which contains high-grade metamorphic schists, gneisses, marble and migmatites metamorphosed in the mid-Cenozoic prior to 60 Ma and around 30 Ma then exhumed by about 20 Ma (Searle et al., 2007).

The Central Troughs (Burma Micro Plate) west of the 1200 km right lateral strike–slip Sagaing Fault comprises sedimentary basins with late Cretaceous and younger sediments thought to be formed above a steep

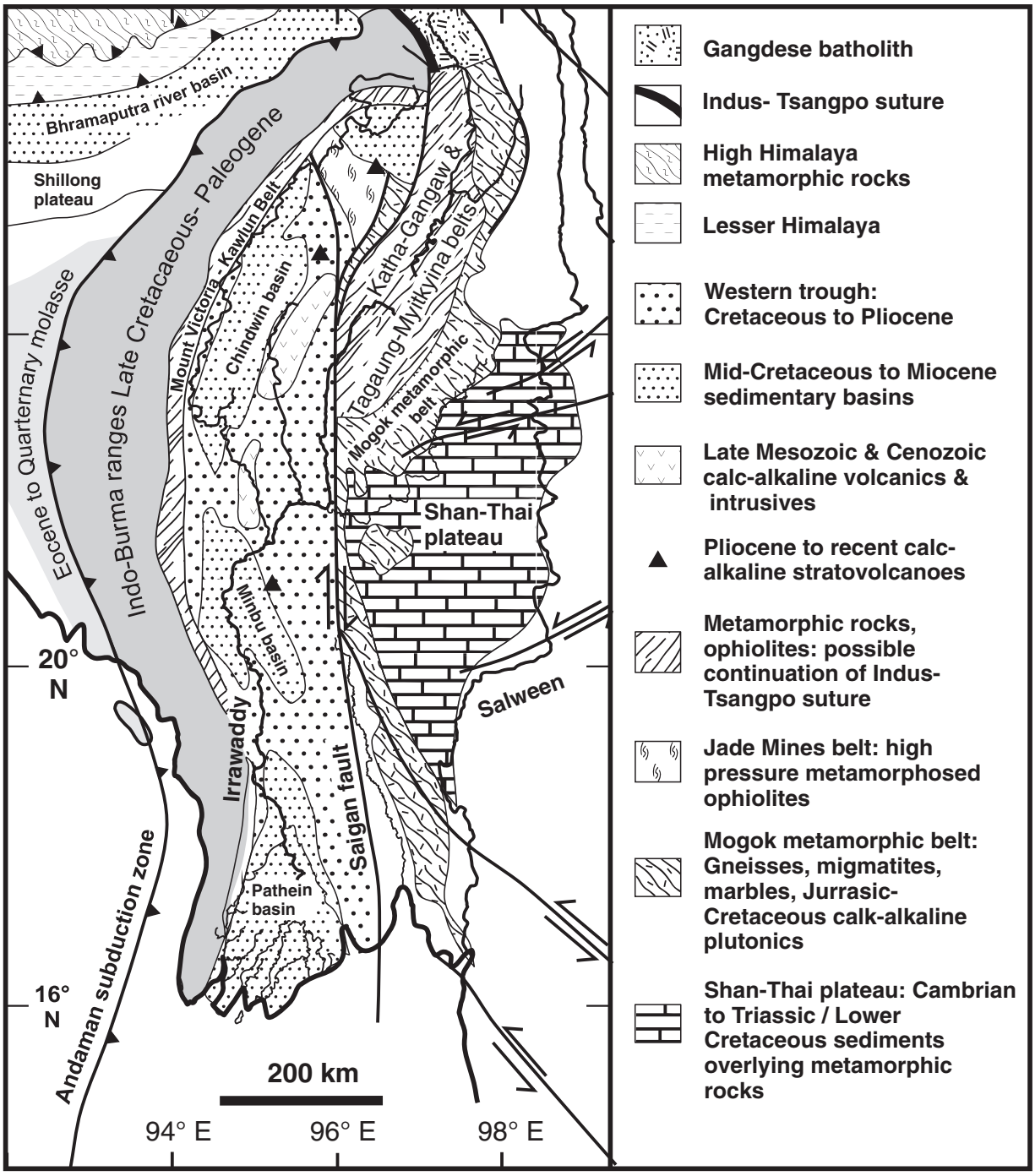

Fig. 3. Geology of Myanmar redrawn from Mitchell et al. (2007) and Searle et al. (2007).

eastwardly dipping subduction zone with associated granite–granodiorite intrusions and alkaline andesite–dacite strato-volcanoes.

The Miocene granitic rocks extend from south of Mandalay through the Shan Scarps, where they are cut by the Salween River, towards south Thailand. These intrusions have been analysed by Darbyshire and Swainbank (1988) giving mainly ages of ~150–100 Ma with present day $^{87}Sr/^{86}Sr$ ratios 0.712–0.717 and are thought to be emplaced during extension after crustal thickening. The Holocene volcanics have lower initial $^{87}Sr/^{86}Sr$ ratios (~0.705) implying a more mantle derived source (Darbyshire and Swainbank, 1988).

The western Indo-Burman Ranges comprise Upper Triassic flysch-type turbidites with some ophiolites, unconformably overlain by Cretaceous to Eocene and younger sediments, mainly limestones with intercalated serpentine sheets. The West Chin Hills may represent a magmatic arc with Eocene ophiolites.

The dextral strike–slip Sagaing fault is thought to separate the Late Oligocene collision of a north facing oceanic arc system with the forearc of west Sumatra (Daly et al., 1991).

The sediments of the upper Irrawaddy basin include volcanics from a Cretaceous arc and sediments shed during the collision (Stephenson and Marshall, 1984; Maury et al., 2004; Najman et al., 2004; Szulc et al., 2006; Allen et al., 2008) as well as subduction related intrusive igneous rocks post-collision (Darbyshire and Swainbank, 1988). The Indo-Burman hills to the west of the Irrawaddy are comprised of the Neogene sedimentary rocks in the west, separated from Palaeogene sediments with local ophiolites and metamorphic rocks of Triassic to

Cretaceous age by the Kaladan Fault. The Indo-Burman hills accreted as forearc flysh above the Sunda Arc subduction zone (Allen et al., 2008).

4. Sampling and analytical methods

Samples for the four time-series were collected fortnightly for periods between September 2004 and March 2007 to cover the entire hydrographic range. These four time series were collected from: 1) Upstream Irrawaddy at Myitkyina [ARW], 2) the main tributary, the Chindwin at Monywa [MNY], 3) downstream Irrawaddy at Hinthada [HTD] and 4) the Salween at Hpa-An close to its entry to the Andaman Sea [THN]. Twenty eight of the main tributaries of the Irrawaddy were sampled in September 2007 along the east bank between Yangon and just north of Mandalay [RA]. Locations are given in Fig. 2.

The four time series water samples were collected by local employees of the Department of Meteorology & Hydrology, Yangon, and the tributary samples by the first two authors. The time series were collected at gauging stations and the collection sites of the tributaries, depending on the size of the tributary were from riverbanks, by lowering a bucket from the centre of bridges or from various sizes of boat. Water samples were filtered on site with 0.2 μm pore size, nylon, Whatman filters. Samples for cations and Sr isotopic analyses were acidified on site with sub-boiling quartz distilled hydrochloric acid to maintain a pH <2. Duplicate samples were left unacidified for anion measurements.

The acidified filtered water samples were analysed for the elements Na, K, Ca, Mg, Si, S and Sr on an inductively coupled plasma-atomic emission spectroscopy Varian VISTA ICP-AES at Cambridge following the method given in de Villiers et al. (2002) using a mixed standard made up from ICP-MS standards with cation proportions specifically designed to match the waters to minimise matrix effects. All samples were analysed in two separate runs with reproducibility within 2%. Anions were analysed on the Dionex ICS-3000 ion chromatograph at Cambridge where repeat measurements of USGS natural river water standard T-143 gave reproducibility better than 4% (2SD, $n = 97$) for the elements (Cl, S, F, N). S measured by emission spectroscopy and ion chromatography reproduced with a mean standard deviation of ~4%. Strontium was separated using Dowex 50Wx8 cation exchange resin with 200–400 mesh particle size in ultra-clean lab conditions and $^{87}Sr/^{86}Sr$ ratios were measured on a VG Sector 54 solid source mass-spectrometer using triple-collector dynamic algorithm, normalised to $^{88}Sr/^{86}Sr$ 0.1194 with an exponential fractionation correction (cf. Bickle et al., 2003; Bickle et al., 2005). The 90 analyses of NBS 987 during the two year period of these analyses gave a mean value of 0.710266 +/− 8 ppm (1 sigma). Blanks were <200 pg and negligible for the Sr concentration of these waters.

5. Elemental concentration results

Concentrations (μmole/l) of cations, anions and the Sr isotopic ratios of all water samples are given in the supplementary data (Table S1). Eleven samples out of the 171 collected have exceptionally high Na, Cl, Ca or Sr concentrations. These include three tributaries with low flows which are considered contaminated as collected close to villages (RA23, 24, 25 which have Na > 19 mmolar), three samples from the Upper Irrawaddy (ARW20 which has Na and Cl a factor of 10 and Sr a factor of 5 greater than the seasonal trend, ARW24 and 28 which have Cl a factor of 4 greater than the seasonal trend), two from the Chindwin (MNY 27, 32 which have Cl a factor of 2 greater than the seasonal trend) and three from the Lower Irrawaddy (HTD 19, 21, 24 which have Cl a factor of 5 to 30 greater than the seasonal trend and low or negative calculated HCO_3^-). These samples have not been included in the following calculations and discussion. Since sampling was often under less than ideal conditions it is likely the high Na and Cl resulted from contamination. Although evaporite deposits or saline brine inputs might impact some of the tributary sample sites, sudden order of magnitude changes in concentrations in the fortnightly samples at the fixed time series collection points in large rivers seem unlikely to be due to changes in water sources. The changes could conceivably reflect run-off from fertilised agricultural land or other anthropogenic additions. It is interesting to note that the single previously published concentration for Na in the Irrawaddy of 1304 μmole/l (Meybeck and Ragu, 1996) is considerably higher than the discharge-weighted mean of our time series at the Lower Irrawaddy of 276 μmol/l with a range of 174–516 μmol/l Na (uncorrected values). The Upper Irrawaddy gives a lower discharge-weighted mean Na concentration of 108 μmol/l Na (range 56–421 μmol/l). The time-series samples from the Chindwin have a discharge-weighted mean Na concentration of 360 μmol/l Na with a range from 229 to a few values as high as 1429 μmol/l during the low flow of January–February. The Salween time series has a discharge-weighted mean Na concentration of 157 (range 81–320) μmol/l which is comparable to the analysis of the Salween of 435 μmol/l published in Meybeck and Ragu (1996), and quoted in Gaillardet et al. (1999) but the Cl concentration of 571 μmol/l quoted by Meybeck and Ragu is over an order of magnitude higher than the discharge-weighted mean Cl of 33 μmol/l (range 3 to 102 μmol/l) in the time-series set. The tributaries to the Irrawaddy, collected during the late monsoon, have lower Na and Cl concentrations than the mainstem with the few higher values in samples collected from shallower streams flowing close to settlements.

6. Correction for cyclic inputs

To investigate weathering fluxes it is necessary to correct the water elemental concentrations for effects of any input from rain, windborne salt, evaporites and hot springs. The compositions of the water samples are corrected for cyclic inputs based on the conservative behaviour of chlorine. A sample of rain (RA1) collected by the Department of Meteorology and Hydrology in August 2007 at a time of high precipitation gave cation and anion concentrations in the same range as rain and snow in the Himalayas but rather lower than rain collected in the Ganges plains which is presumed concentrated by evapotranspiration (Galy and France-Lanord, 1999). The sample (RA1) has a low Na/Cl of 0.51 with 4.5 μmol/l Cl. However the low sodium concentration in Yangon may not reflect the nationwide aerosol Na/Cl ratio. The composition of the rain involves contributions from windborne oceanic salt and carbonate and silicate dust as well as the effects of evapotranspiration and is likely to exhibit significant temporal and spatial variations (Krishnamurthy and Bhattacharya, 1991; Alford, 1992; Galy and France-Lanord, 1999; Bickle et al., 2005). All data are corrected for cyclic inputs assuming the rain contains 28 μmolar Cl with Na/Cl = 0.87, Ca/Na = 0.02 and Mg/Na = 0.11, the values of mean ocean water and natural salt compositions. The remaining Cl is assumed to be derived from evaporite sources and the cation concentrations are corrected using the mean evaporite compositions compiled by Gaillardet et al. (1999) with Na/Cl = 0.84, Ca/Na = 0.19 and Mg/Na = 0.025 and Sr/Cl = 1.31×10^{-3}. The correction for Na is on average 20% of sample concentration. For a subset of samples from Monywa on the Chindwin tributary with higher Cl concentrations, the Na correction averages 33%. Corrections for the other cations are much smaller.

7. Averaging, interpolation and calculation of uncertainties

Monthly averages of the river samples corrected for cyclic inputs, calculated from the data which spans the years 2004 to 2007, illustrate the seasonal variability of the weathering chemistries while smoothing short timescale variability and allow calculation of the mean annual chemical fluxes (Fig. 4). The water sampling at two-week intervals over the period 2004–2007 has significant gaps, most notably there were no usable samples collected in either April or July on the Lower Irrawaddy and Chindwin, July and August on the Salween, and July on

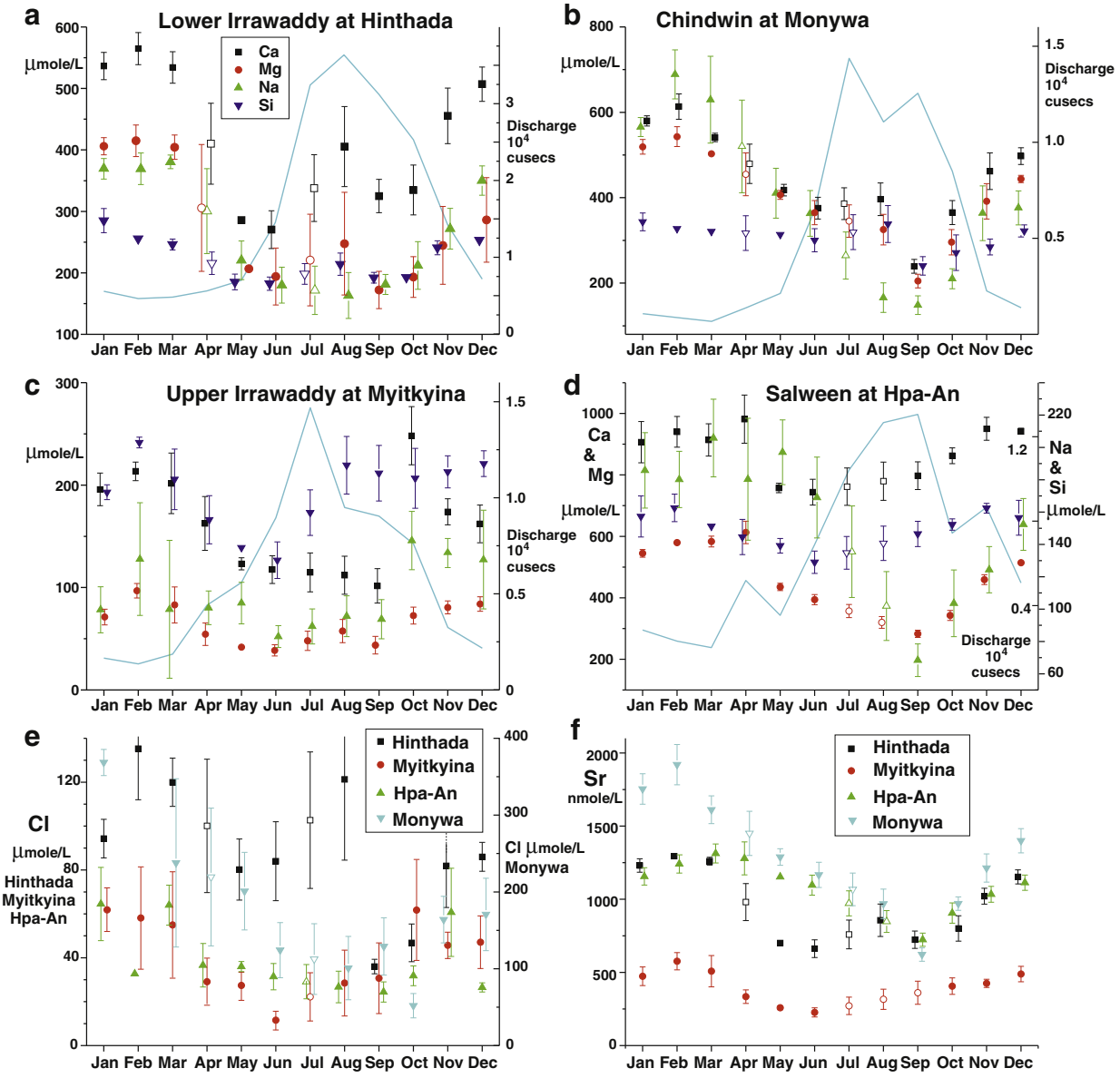

Fig. 4. a, b, c & d. Average monthly Ca, Mg, Na, Si concentrations, corrected for cyclic inputs, at Hinthada (Lower Irrawaddy), Monywa (Chindwin), Myitkyina (Upper Irrawaddy) and Hpa-An (Salween). e & f. Monthly Cl and Sr concentrations at time series sample sites. Error bars 1 × standard errors (see text) but not shown where smaller than symbols. Open symbols are months with no samples and the values shown are interpolated between adjacent sampled months and are used in calculating annual fluxes. Blue line in a is average monthly discharge at Pyay from Robinson et al. (2007) in cusecs and blue line in b, c & d are monthly discharge from 2004 data. Note discharge values for winter months in Salween interpolated as discussed in text. (For interpretation of the references to colour in this figure legend, the reader is referred to the web version of this article.)

the Upper Irrawaddy. In order to calculate annual fluxes, values have been interpolated between adjacent months where data is missing.

Uncertainties (one standard error on mean) have been calculated for all the months with 3 or more samples. The uncertainties on the months with one or two samples have been derived by first calculating the mean fractional standard deviation (σ_f) for all the months with 3 or more samples as

$$\sigma_f^2 = \frac{\sum_i (n_i - 1)\sigma_i^2/\overline{x_i}}{\left(\sum_i n_i - 1\right)} \quad (1)$$

where σ_i is standard deviation of the n_i samples in month 'i', mean concentration, $\overline{x}_i$. It is then assumed that σ_f is the uncertainty on months with one sample or months without analyses and $\sigma_f/\sqrt{2}$ is the uncertainty on the mean concentration for months with two samples (Fig. 4).

8. Variation in concentration with time of year

The significant changes in river flow throughout each year due to the monsoon climate experienced by this region have a major effect on elemental concentrations in each river. Water flow is significantly higher during the monsoon, which although variable in date from year to year, starts around June and extends until the end of October. The monthly precipitation at Yangon and Mandalay is shown in Fig. 5 (New et al., 2002).

In the Irrawaddy, monsoon rains increase discharge by a factor of ~7 from an average of ~12 km^3/month in the dry months (November to April) to ~89 km^3/month in August at the height of the monsoon (Robinson et al., 2007). Fig. 4 illustrates that the corresponding dilution

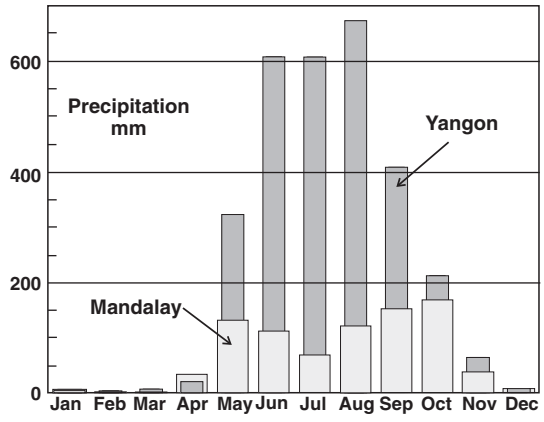

Fig. 5. Average monthly precipitation at Yangon & Mandalay after New et al. (2002).

in the elemental concentrations is damped with a factor of 2 to 3 decrease in Na, Ca, Mg and Sr, a factor of 1.5 decrease in Si but virtually no change in K concentrations during the monsoon. The Upper Irrawaddy and the Chindwin exhibit similar decreases in concentrations. The Salween exhibits more muted dilutions with Na decreasing by a factor of 2, Ca, Mg, K and Sr decreasing by factors between 1.2 and 1.4, and Si showing a minor reduction. The Salween also contains twice the Ca content with average 832 μmol/l Ca compared to 370 μmol/l Ca for the Lower Irrawaddy. The Upper Irrawaddy (ARW) and the Salween (THN) have lower chlorine contents concomitant with lower evapotranspiration at their higher altitudes and locations.

All the sample suites exhibit a similar hysteresis in the variation of cation concentrations with discharge. Fig. 6a illustrates Ca and Sr concentrations versus discharge (Q) for the Lower Irrawaddy. This exhibits high concentrations during the low flow months November to April, a decrease in concentrations as discharge increases through May and June, but then a small increase in concentrations during the high discharge months of July to October. Fig. 6b, which illustrates the variations in 1000 x Sr/Ca (hereafter written as Sr/Ca) and Na/Ca ratios with discharge, shows that the ratios increase during the low discharge months from November to May but then decrease through June to the highest discharge months of July to September. These mismatches between concentrations, element ratios and discharge imply seasonal changes in the relative contributions from differing sources and/or changes in weathering mechanisms (cf. Anderson et al., 1997; Tipper et al., 2006).

9. Weathering inputs

Calcium concentrations decrease less during the monsoon than sodium, magnesium and strontium (Figs. 4 & 7). The changes in chemistry in these large catchments may either reflect changes in the relative inputs from different parts of the catchments, different proportions of water sources (eg. shallow to deep groundwaters) or changes in weathering mechanisms. The decrease in Na/Ca, Sr/Ca and Mg/Ca ratios is consistent with greater inputs from carbonates during the monsoon. However Si/Ca ratios only decrease during the monsoon in the Upper Irrawaddy at Myitkyina. It is possible that Si in the Chindwin and the Salween is buffered by variable biological uptake or release, by release of adsorbed Si on iron oxy-hydroxide minerals or more complex precipitation/dissolution reactions with silicate minerals (Fontorbe et al., 2013).

Similar changes in the relative inputs from silicate and carbonate minerals have been observed in a number of Himalayan catchments and Taiwanese rivers (Tipper et al., 2006; Calmels et al., 2011) and these have been attributed to a greater contribution of deeper groundwaters at times of low flow contrasting with rapid runoff of surface waters and shallow groundwaters at times of high flow. The rapid runoff is thought to have a relatively high carbonate contribution, reflecting the much more rapid dissolution kinetics of carbonate and the shorter water residence time in the weathering zone, whereas deeper groundwaters become more enriched in silicate-derived components. Tipper et al. (2006) and Calmels et al. (2011), following Galy and France-Lanord (1999), Jacobson et al. (2002) and (Bickle et al., 2005), argue that the Himalayan and Taiwanese waters have lost a significant fraction (up to ~70%) of their Ca to precipitation of secondary calcite. The high 1000 × Sr/Ca molar ratios (1.5 to 2.2) for the carbonate inputs to the Irrawaddy and Chindwin inferred from extrapolation of the correlations on a plot of Sr/Ca versus Na/Ca (Fig. 8—see also Bickle et al., 2005) are much higher than the Sr/Ca ratios of most carbonate rocks which are less than 1.0 (Jacobson et al., 2002; Bickle et al., 2005) and imply comparable magnitudes of precipitation of secondary calcite. The Salween has a much lower Sr/Ca intercept (~0.6) and lower Sr/Ca ratios (Fig. 8a); the contrasting controls on its water chemistry are discussed further below. The Lower Irrawaddy samples from Hinthada plot between the upstream samples of the Irrawaddy at Myitkyina, which have a similar range in Na/Ca, the Irrawaddy floodplain tributaries, most of which have higher Na/Ca and the Chindwin samples which plot at slightly higher Sr/Ca over a similar range of Na/Ca (Fig. 8b). The four most northern floodplain samples collected from tributaries which rise in the Shan-Thai plateau and Mogok metamorphic belt have low Na/Ca and Sr/Ca indicative of carbonate inputs. Two of these samples have elevated

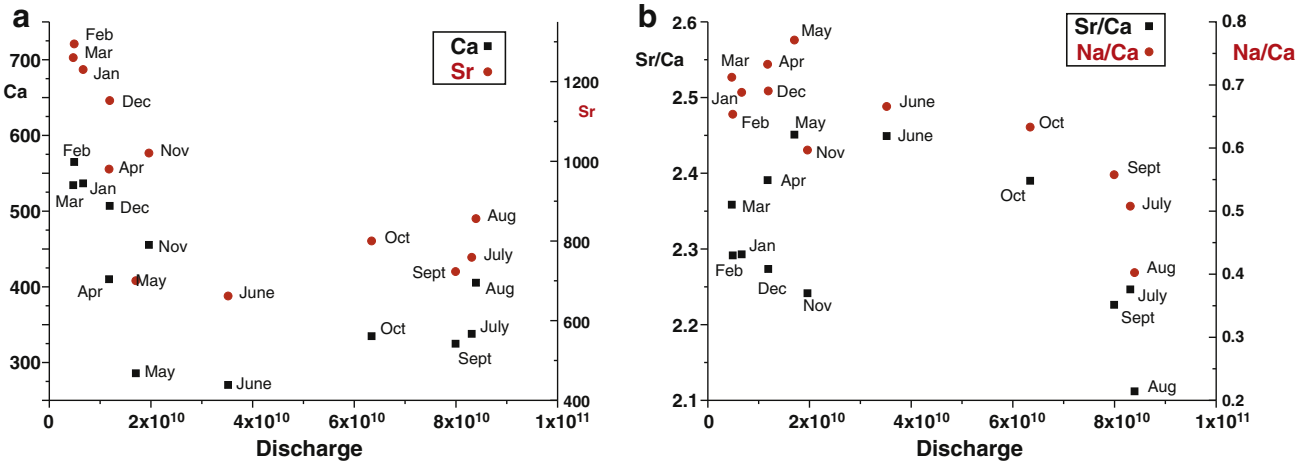

Fig. 6. Mean monthly Ca and Sr concentrations (a) and mean monthly 1000 x Sr/Ca and Na/Ca ratios (b), corrected for cyclic inputs, at Hinthada (Lower Irrawaddy) plotted against the mean monthly discharge (m^3/month) at Pyay from Robinson et al. (2007).

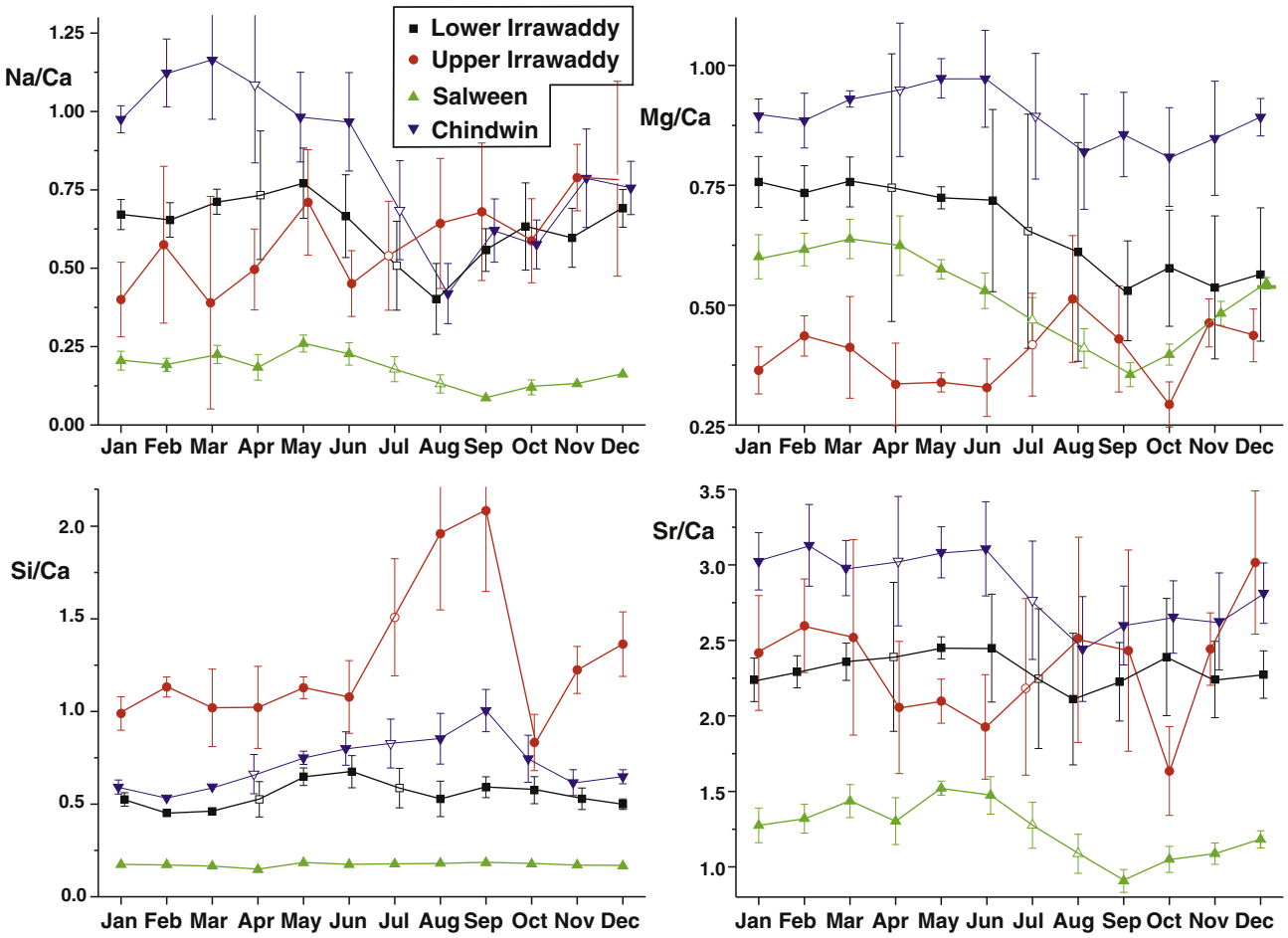

Fig. 7. Mean monthly Na/Ca, Mg/Ca, Si/Ca and Sr/Ca ratios (corrected for cyclic inputs) at four time-series sample sites. Error bars 1× standard errors on mean values. Open symbols are months with no samples and values are interpolated between adjacent sampled months.

$^{87}Sr/^{86}Sr$ ratios expected from the older rocks in the Mogok metamorphic belt. The other tributaries and the Chindwin samples have a similar range of relatively low $^{87}Sr/^{86}Sr$ ratios consistent with the young, arc derived sediments of the Indo-Burman ranges (Fig. 9d). One floodplain tributary, which rises near the volcanic centre Mt Popa has a very low $^{87}Sr/^{86}Sr$ ratio of ~0.705.

The secular variations in Sr-isotopic composition for the Lower Irrawaddy and Chindwin sample sites are broadly consistent with the changes in elemental ratios. The marked drops in $^{87}Sr/^{86}Sr$ over the monsoon are attributed to an increased contribution of Sr from carbonate with low $^{87}Sr/^{86}Sr$ ratios (Fig. 9a). The Upper Irrawaddy exhibits a marked increase in $^{87}Sr/^{86}Sr$ ratios from January to June while the Sr/Ca and Na/Ca ratios fall (Fig. 7) indicative of an increased fraction of these ions from weathering of carbonate. It is probable that this reflects changing inputs from the contrasting geological terrains drained by this river with rainfall patterns shifting to the north-east prior to the

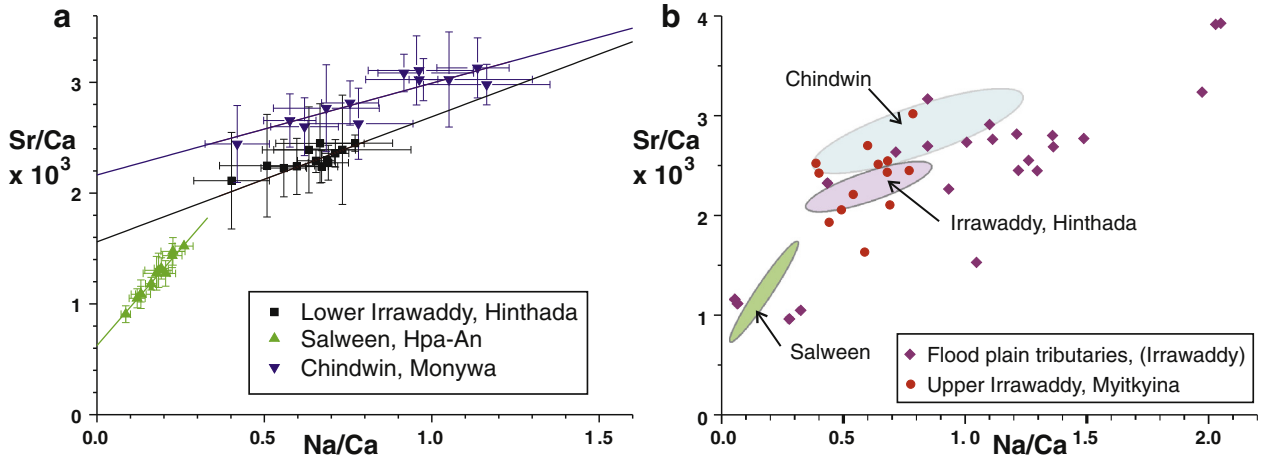

Fig. 8. a. Sr/Ca versus Na/Ca ratios for cyclic-corrected mean monthly samples from Lower Irrawaddy at Hinthada, Salween at Hpa-An and Chindwin at Monya. Lines are least squares best fits to arrays. b. Sr/Ca versus Na/Ca ratios for Irrawaddy floodplain tributaries compared to fields for Lower Irrawaddy at Hinthada, Salween at Hpa-An and Chindwin at Monywa.

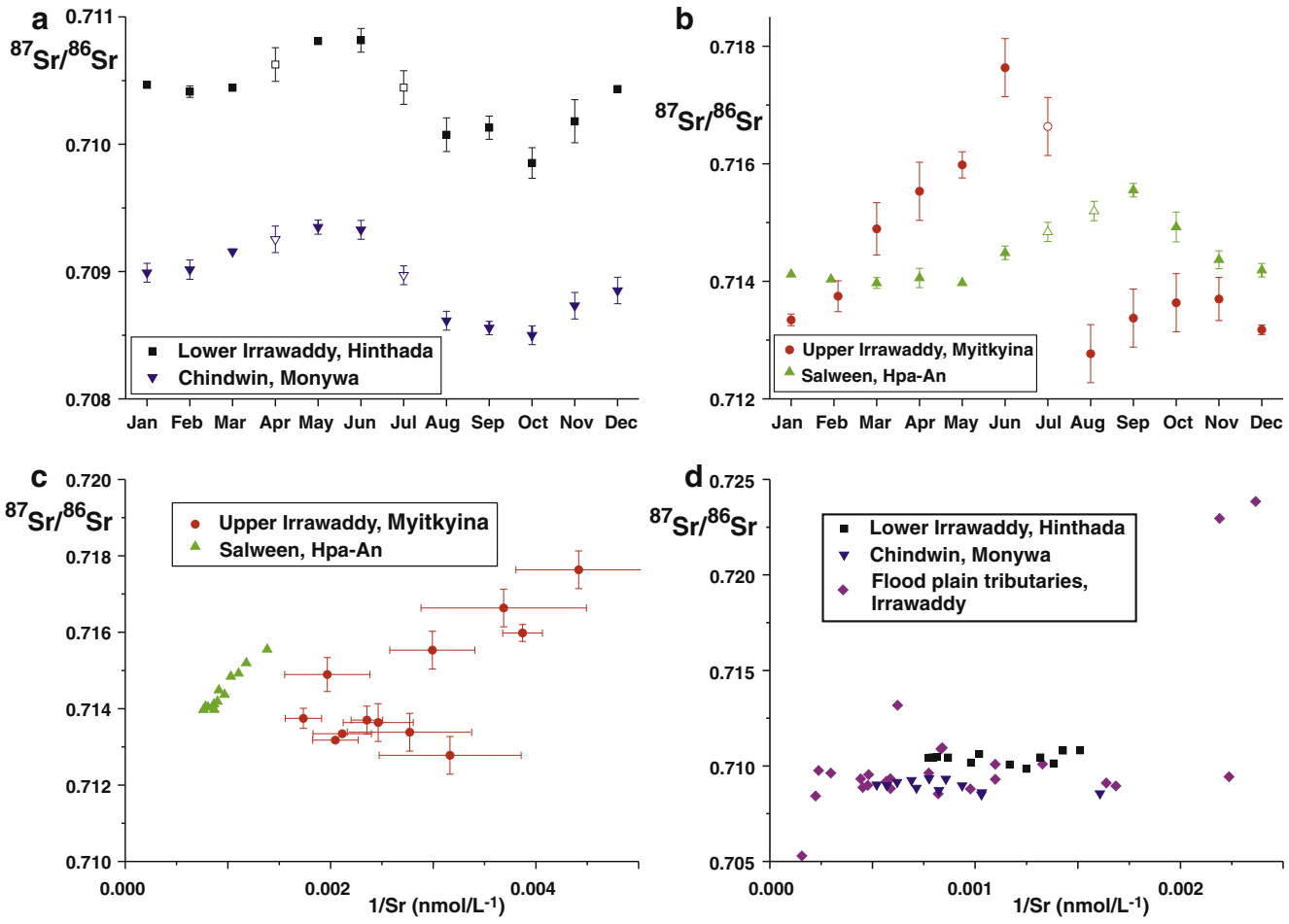

Fig. 9. (a) and (b) show variation of mean monthly $^{87}Sr/^{86}Sr$ ratios from Irrawaddy at Hinthada, Salween at Hpa-An, Chindwin at Monya and Irrawaddy at Myitkyina. Note that the Salween at Hpa-An and Irrawaddy at Myitkyina have higher $^{87}Sr/^{86}Sr$ ratios reflecting inputs from the older basement to the east and the Himalayan ranges. (c) and (d) show mean monthly $^{87}Sr/^{86}Sr$ ratios versus 1/Sr for Irrawaddy at Myitkyina and Salween at Hpa-An, Irrawaddy at Hinthada, Chindwin at Monya and floodplain tributaries. Error bars 1 × standard errors (see text) but not shown where smaller than symbols. The positive correlations exhibited by the Salween at Hpa-An and Irrawaddy at Myitkyina probably reflect dilution of Sr concentrations in the monsoon coupled with a greater input from more northerly, more radiogenic, catchments. The two high $^{87}Sr/^{86}Sr$ ratio samples are from flooded fields and the adjacent Chaungmagyi River which drains the Mogok metamorphic rocks.

monsoon causing increasing inputs from the older rocks of the Asian plate. The Palaeozoic rocks of the Asian plate and the Mogok Metamorphic Belt to the east have higher $^{87}Sr/^{86}Sr$ ratios than the younger accretionary complex Indo-Burman Ranges to the west which is reflected in the higher $^{87}Sr/^{86}Sr$ ratios in the Upper Irrawaddy time-series set (0.7128 to 0.7176) compared with the Chindwin (0.7085 to 0.7095) which only drains the Indo-Burman Ranges (Fig. 3). The Asian plate rocks are heterogeneous with some Cretaceous igneous volcanics and intrusions exhibiting low initial Sr isotopic ratios (I-type granitoids 0.7058 – 0.7063 and S-type granodiorites 0.7126 – 0.7158, Darbyshire and Swainbank, 1988). However much of the terrain is older basement with higher $^{87}Sr/^{86}Sr$ ratios such as from Yezin Dam at 0.747 in the Shan Scarp region and similar for the Sungei Makaung rhyolite with $^{87}Sr/^{86}Sr$ ratios of 0.746 in the Central Valley (Darbyshire and Swainbank, 1988; see also Mitchell et al., 2012). Radiogenic inputs from these terrains are confirmed with an $^{87}Sr/^{86}Sr$ ratio of 0.7238 in sample RA30 from a tributary north of Mandalay.

The Salween, by contrast, exhibits an increase in $^{87}Sr/^{86}Sr$ ratios over the monsoon while Na/Ca and Sr/Ca ratios decrease (Figs. 8 & 9b). This is likely to be due to increased inputs from Tibet and the Himalayas as the rains penetrate north at the height of the monsoon. The Sr-isotopic composition of the Salween in Tibet was measured in September 2003 at 0.71274 (Tipper et al., 2010). However the Sr inputs from rivers draining Himalayan metamorphic rocks are markedly more radiogenic and by analogy with the other rivers draining the Himalayas and Tibet (e.g. Harris et al., 1998; Galy and France-Lanord, 1999; Bickle et al., 2003), these inputs would be characterised by both a dominant contribution from carbonate minerals and $^{87}Sr/^{86}Sr$ ratios as high as 0.74. The samples from the Salween and Upper Irrawaddy, averaged by month, exhibit good positive correlations on a plot of $^{87}Sr/^{86}Sr$ versus 1/Sr (Fig. 9c) normally interpreted to represent mixing between a low $^{87}Sr/^{86}Sr$, high Sr (ie low 1/Sr) carbonate component and a high $^{87}Sr/^{86}Sr$, low Sr silicate component. Here the correlations may reflect mixing between a component from the lower reaches of the river with lower $^{87}Sr/^{86}Sr$ but high Sr at times of low flow dominant during the winter and a higher $^{87}Sr/^{86}Sr$ component supplied by the high $^{87}Sr/^{86}Sr$ ratio Himalayan carbonates but at low Sr concentrations diluted by the high flow during the summer.

10. Chemical fluxes delivered by the Irrawaddy and the Salween

The chemical weathering fluxes from the Lower Irrawaddy, the Chindwin, the Upper Irrawaddy and the Salween, corrected for cyclic inputs, have been calculated from the monthly averaged chemical data and uncertainties, interpolated where necessary. Monthly water discharge for the downstream Irrawaddy site at Hinthada have been taken as the mean of the 10 or 11 years sampling between 1869 and 1879 by Gordon (1879–1880) at Pyay, 130 km upstream of Hinthada, published and corrected by Robinson et al. (2007). Discharge for the Upper Irrawaddy site at Myitkyina, the Chindwin and the Salween

have been taken from the monthly water flux data for 2004 published by the Dept. Hydrology and Meteorology, Rangoon (see supplementary data, Table S2). Discharge data for the Salween at Hpa-An is only available for the months of May to October in 2004, measured by the Department of Hydrology and Meteorology, Rangoon. The values for the remaining months have been calculated by assuming that their cumulate discharge is the difference between the 2004 May to October discharge and the annual discharge of 211 km^3/yr quoted by Meybeck and Ragu (1996). This discharge is apportioned to the months January to March and November and December in the same proportions as the mean monthly discharge in the Irrawaddy at Pyay. The monthly 2004 water flux data at Hinthada (Dept. Hydrology and Meteorology, Rangoon) differs by between 2 and 50% from the 10/11 year averages of Robinson et al. (2007) with the largest discrepancies in April, May and November. These differences are within the expected variability from the 10 or 11 year sampling of the Gordon data.

The cation fluxes are illustrated in Fig. 10. The 1σ uncertainties on the monthly fluxes (supplementary data Table S2) have been calculated by combining the uncertainties on the mean monthly concentrations discussed above and the standard deviations of the monthly discharge data calculated from the 10 or 11 year sampling by Gordon, assuming that the chemistry and discharge are uncorrelated. Where chemical data is averaged over months from two or three years the uncertainty on the monthly discharge is taken as the standard deviation for that month divided by $\sqrt{2}$ or $\sqrt{3}$. It is assumed that the uncertainties on the monthly fluxes on the Upper Irrawaddy, the Chindwin and the Salween are the same as those calculated for the Irrawaddy at Pyay from Gordon's data. The 1σ uncertainties on the annual fluxes (Fig. 10, Table S2) have been calculated by a Monte Carlo routine which takes into account the uncertainties on the monthly average chemical concentrations and the monthly discharge data. The Sr flux-weighted mean annual Sr-isotopic composition and uncertainty are calculated by the same programme.

The five monsoon months (June to October) dominate the chemical fluxes contributing between 70% and 80% of the elemental fluxes in the Irrawaddy sample sites and between 45% and 54% of the elemental fluxes in the Salween. The Chindwin and the Upper Irrawaddy together contribute 85% of the water flux and between 60% and 70% of the elemental fluxes of the downstream sample site at Hinthada. Si is an exception, showing a decrease reinforcing the conclusion that Si behaviour is non-conservative, plausibly related to biological uptake.

11. Ratio of silicate to carbonate inputs

It is the silicate-derived cation fluxes that impact long-term climate. Discriminating the fractions of Ca and Mg derived from silicate minerals from the much larger components derived from carbonate minerals is problematic. Here we calculate silicate derived Ca and Mg using a forward model based on the estimated end member Ca/Na and Mg/Na ratios in silicate rocks from Gaillardet et al. (1999) of $Ca/Na^* = 0.35 \pm 0.15$ and $Mg/Na^* = 0.24 \pm 0.12$, where Na^* is the value corrected for saline inputs (see review of methods by Moon et al., 2014). The comparison of the silicate-derived cations in the Irrawaddy and Salween to global fluxes is restricted to the Ca and Mg components because magnitude of reverse weathering and thus the fate of alkalinity

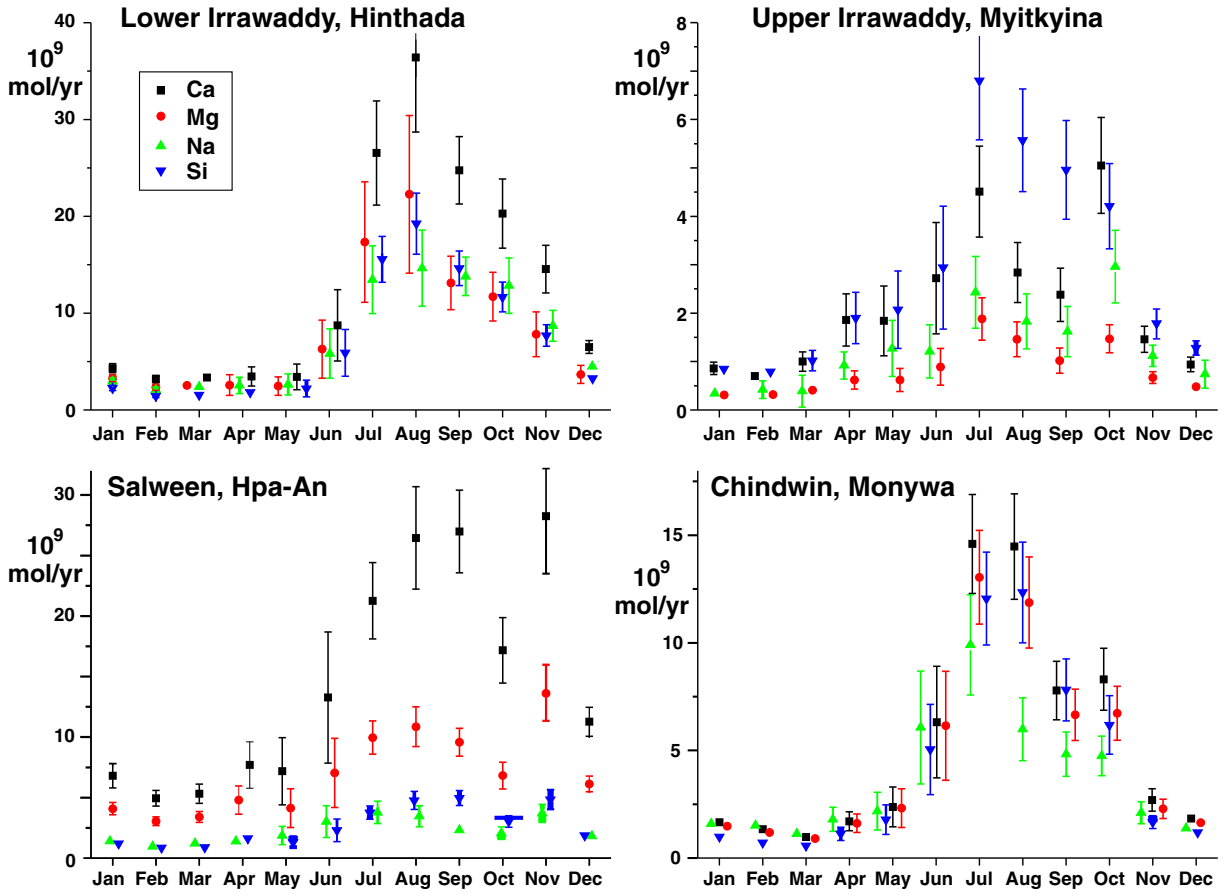

Fig. 10. Ca, Mg, Na and Si monthly fluxes in the Irrawaddy at Hinthada, Irrawaddy at Myitkyina, Salween at Hpa-An and the Chindwin at Monya. Error bars are the combined uncertainty from 1 standard error on the concentration mean of samples included in the monthly average or estimated from the mean error from months with more than two samples (see text and Eq. 1) and the uncertainty in the monthly discharge fluxes as discussed in the text.

associated with Na and K in the ocean is uncertain (e.g. Michalopoulos and Aller, 1995).

The dissolved Ca plus Mg load from the Irrawaddy River, (Upper, Lower and the Chindwin Tributary), is close to 80% carbonate-derived and 20% silicate-derived whilst the Salween has a higher carbonate influence with up to 94% of the Ca plus Mg derived from carbonate and only 6% from silicate rocks (Table 1).

The monthly average Chindwin samples exhibit a good correlation between the $^{87}Sr/^{86}Sr$ ratios and the percentage of Ca derived from silicates (Fig. 11a) consistent with the expected higher $^{87}Sr/^{86}Sr$ ratio of silicates compared to carbonates and the correlation with Na/Ca ratios discussed above. The Upper Irrawaddy is more variable (Fig. 11b) probably reflecting temporal changes in inputs from the higher $^{87}Sr/^{86}Sr$ ratio metamorphic rocks of the Moguk belt and Asian plate and lower $^{87}Sr/^{86}Sr$ ratio rocks of the western Indo-Burman Ranges. The Irrawaddy at Hinthada exhibits a poor positive correlation between the $^{87}Sr/^{86}Sr$ ratios and the percentage of Ca derived from silicates and $^{87}Sr/^{86}Sr$ ratios intermediate between those of the Chindwin and the Upper Irrawaddy sample set consistent with being a mixture of the two (Fig. 11a). The Salween River exhibits a negative correlation (Fig. 11b) as expected from the negative correlation between $^{87}Sr/^{86}Sr$ ratios and Ca/Na discussed above and thought to reflect inputs dominated by the Himalayas at high flow during the monsoon and by the lower reaches during the winter.

12. Riverine chemical weathering fluxes from Himalayan–Tibetan orogen

Water discharge from the Irrawaddy and Salween total 633 km^3/yr which is about 20% of the overall water discharge from the Himalayan–Tibetan orogeny (Table 1). The catchment area of the Irrawaddy covers 0.3%, and the Salween 0.2%, of global continental area and combined, they comprise about 10% of catchment areas of the main rivers draining the Himalayan–Tibetan orogen.

These values compare with the Ganges which drains an area equal to the Irrawaddy and Salween combined (0.7% of continental area) but has a lower discharge (380 km^3/yr, 1.0% of global). The Brahmaputra also has a comparable discharge (690 km^3/yr, 1.8% of global) but from only 0.4% of global continental area.

The bicarbonate flux associated with cations derived from silicate minerals is important for its control on climate change. Mg is quantitatively exchanged for Ca in the oceanic crust and the fractions of Ca and Mg derived from bicarbonate weathering of silicate minerals contribute to removal of CO_2 from the atmosphere deposited as limestone in the oceans. The fate of Na and K is less certain with some exchanged for Ca in the oceanic crust and some lost to reverse weathering with the CO_2 returned to the atmosphere (e.g. Michalopoulos and Aller, 1995). We therefore compare the annual silicate-derived Ca + Mg flux from the Irrawaddy and Salween and from the whole area of the Himalayan–Tibetan orogeny with the global silicate-derived Ca + Mg flux calculated from the compilation of Gaillardet et al. (1999), given the revisions and additions to rivers draining the Himalayan–Tibetan region detailed in Table 1. The annual Ca + Mg flux derived from silicates previously calculated for the Irrawaddy appears unreliable as the discharge-weighted mean Na of the data here (276 μmol/l) is only 20% of the value of 1304 μmolar quoted by Meybeck and Ragu (1996). The fluxes of Ca + Mg derived from silicate minerals for the Irrawaddy and Salween of 5.1×10^{10} and 1.6×10^{10} mol/yr give global contributions of 2.5% and 0.8% respectively (Table 1). This major contribution is comparable to 2.0% from the Ganges and 1.4% from the Brahmaputra.

Based on 60 major rivers in the world, weathering of silicate minerals supplies about 2046×10^9 mol/yr of Ca + Mg (using data from Gaillardet et al., 1999), and our revised flux from the rivers draining the Himalayan–Tibetan orogeny (Table 1, see also supplementary information Table S3) is 283×10^9 mol/yr, or about 14% of the total. This 14% is derived from only 4.8% of global continental area, emphasising the significance of silicate weathering resulting from the Himalayan–Tibetan orogeny.

These current estimates of the silicate weathering are still subject to a number of important uncertainties. Time series sampling helps overcome variations of river discharge as shown by the revision of the Irrawaddy dissolved discharge in this paper. Increasing sampling of small rivers from volcanic arcs and basaltic oceanic islands, as discussed by Dessert et al. (2003), will lead to better estimates of the poorly sampled volcanic inputs. The partition of the riverine chemical fluxes to the silicate, carbonate, evaporite and rain-derived fractions is still the most problematic aspect of the calculations (e.g. Bickle et al., 2015). Further in the Irrawaddy and Salween 31% and 24% of the anion charge are supplied by sulphate and it is likely that much of this is supplied by oxidation of pyrite which is important in rapidly eroding catchments (c.f. Turchyn et al., 2013; Torres et al., 2014).

13. Strontium signatures of Himalayan–Tibetan Rivers

The Irrawaddy supplies 1.6% and the Salween 1.0% of the global dissolved riverine Sr flux to the oceans and the two rivers contribute ~12%

Table 1
Silicate Ca plus Mg, Sr and ^{87}Sr fluxes from rivers draining the Himalayan–Tibetan region.

	Area 10^6 km^2	Catchment area % land	Discharge km^3 yr^{-1}	Discharge % global[10]	Silicate Ca + Mg flux x 10^9 mol/yr[11]	Silicate Ca + Mg flux % of global	Sr % of global	$^{87}Sr_e$ % of global[12]
Chang Jiang[1]	1.81	1.22	900	2.4	20–54	1.8	10.6	4.2
Brahmaputra[2]	0.58	0.39	690	1.8	16–43	1.4	1.6	8.3
Ganges[3]	1.05	0.71	380	1.0	22–58	2.0	1.6	7.6
Irrawaddy[4]	0.41	0.28	422	1.1	28–74	2.5	1.6	0.5
Salween[4]	0.33	0.22	211	0.6	9–23	0.8	1.0	1.3
Mekong[5]	0.80	0.54	425	1.1	8–20	0.7	0.9	1.0
Indus[6]	0.92	0.62	90	0.2	17–46	1.5	1.1	0.8
Huang He[7]	0.75	0.51	51	0.1	10–27	0.9	2.9	1.6
Hong He[8]	0.12	0.08	123	0.3	3–7	0.2	0.5	0.3
Pearl[9]	0.42	0.28	285	0.8	17–45	1.5	1.0	0.7
Total	7.171	4.8	3576	9.6	148–398	7–20	23	26

Data sources: 1) Chen et al. (2002) except Sr and $^{87}Sr/^{86}Sr$ average of data in Gaillardet et al. (1999) and Wang et al. (2007), 2) data from Galy and France-Lanord (1999) and Galy et al. (1999), Sarin et al. (1989), Krishnaswami et al. (1992) and Singh et al. (2005), 3) data from Galy and France-Lanord (1999) and Galy et al. (1999), Sarin et al. (1989), Krishnaswami et al. (1992), 4) this paper (supplementary data, Table S1), 5) average of samples collected for this study (supplementary data, Table S1), daily discharge weighted average of monthly samples over 1961 and 1962 by Meybeck and Carbonnel (1975) and arithmetic average of monthly sampling between 1972 and 1998 by Li et al. (2014). Sr and $^{87}Sr/^{86}Sr$ ratio this study (Table S1), 6) Gaillardet et al. (1999), 7) Chen et al. (2005) using pre-regulated discharge weighted chemistry (Table 6), 8) summer and winter concentrations weighted by summer and winter discharges from Moon et al. (2007), 9) arithmetic average of sampling between 1958 and 2002 from Zhang et al. (2007), 10) discharge from GRDC database (http://www.bafg.de/GRDC/EN/Home/homepage_node.html) except Irrawaddy and Salween from Robinson et al. (2007), Huang He from Chen et al. (2005) and Pearl from Zhang et al. (2008). 11) Range calculated for assumed silicate Ca/Na ratios of 0.2 to 0.5. 12) $\%^{87}Sr_e$ is percentage of ^{87}Sr flux with $^{87}Sr/^{86}Sr$ ratio in excess of modern seawater which gives the relative forcing on changes in ocean $^{87}Sr/^{86}Sr$ ratios (see text and Bickle et al., 2005).

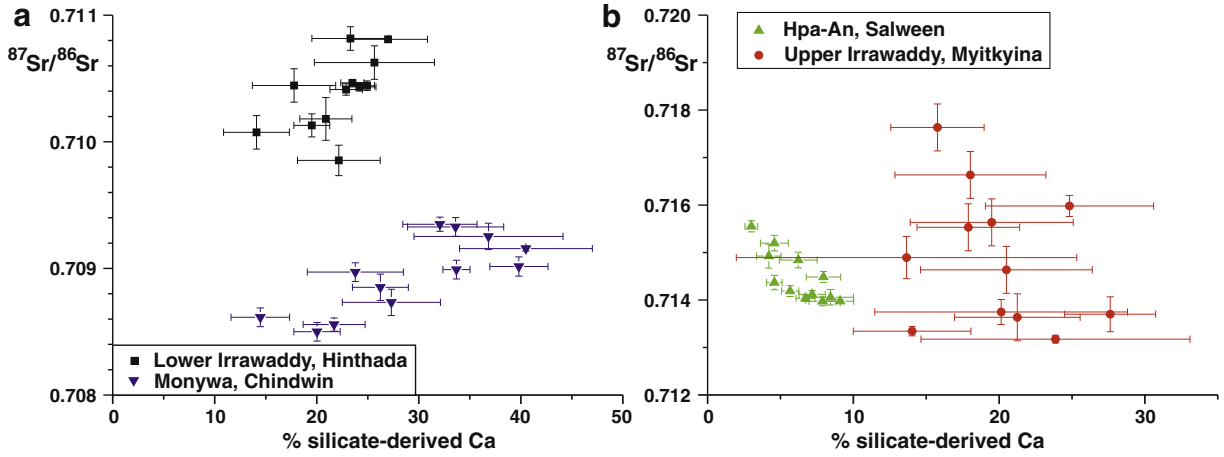

Fig. 11. (a) $^{87}Sr/^{86}Sr$ ratios versus percentage of silicate-derived Ca from the Irrawaddy at Hinthada, and Chindwin at Monya and (b) the Salween at Hpa-An, and Irrawaddy at Myitkyina. Percentage of silicate-derived Ca is calculated by assuming a silicate Na/Ca ratio of 0.35 where Na is that corrected for rain and evaporate inputs as discussed in text. Poor positive correlations for Irrawaddy at Hinthada, and Chindwin at Monya probably reflect an increased proportion of silicate dissolution in the dry season. Scatter exhibited by the Irrawaddy at Myitkyina and the good negative correlation exhibited by the Salween at Hpa-An probably reflect increased inputs of higher $^{87}Sr/^{86}Sr$ ratio carbonates from the metamorphic rocks to the east and north during the monsoon.

of the Sr discharge from the Himalayan–Tibetan region (Table 1). The discharge-weighted mean Sr-isotopic composition of the Irrawaddy at 0.71024 ± 5 is lower, and the Salween at 0.71466 ± 6 (supplementary data Table S2) is only slightly higher than estimates of the average discharge-weighted mean global river $^{87}Sr/^{86}Sr$ ratio. The data in Gaillardet et al. (1999) combined with the revised values in Table 1 give a mean global riverine $^{87}Sr/^{86}Sr$ ratio of 0.7127, whereas Peucker-Ehrenbrink et al. (2010) used relationships between bed-rock age and dissolved $^{87}Sr/^{86}Sr$ ratios to estimate a mean global riverine $^{87}Sr/^{86}Sr$ ratio of 0.711. Despite their relatively large Sr-fluxes, the Irrawaddy and Salween only contribute 1.3% of the riverine forcing of oceanic $^{87}Sr/^{86}Sr$ ratios, compared to the 16% from the Ganges and Brahmaputra. The riverine forcing on oceanic $^{87}Sr/^{86}Sr$ ratios is calculated as the $Sr_{flux}x(^{87}Sr/^{86}Sr_{river}$-0.709). The fraction of the high $^{87}Sr/^{86}Sr$ ratios of the Ganges and Brahmaputra, and by analogy the Salween, supplied by carbonate minerals with their $^{87}Sr/^{86}Sr$ ratios elevated by metamorphic exchange in the Himalayas is still uncertain (cf. Galy et al., 1999; Bickle et al., 2005).

14. Conclusions

This study has determined the chemical and Sr-isotopic fluxes carried by the Irrawaddy and Salween Rivers from the first set of four time series collected from these two major Asian rivers in the Himalayan–Tibetan region.

Both rivers exhibit seasonal variations in the ratio of carbonate to silicate weathering with more carbonate weathering taking place during the monsoon. The Irrawaddy and its tributary the Chindwin exhibit lower $^{87}Sr/^{86}Sr$ and Na/Ca ratios during and immediately post-monsoon, interpreted to reflect higher weathering of carbonate at times of high flow.

The Salween exhibits higher $^{87}Sr/^{86}Sr$ ratios with lower Na/Ca ratios during the monsoon, interpreted to reflect higher inputs from the upper parts of the catchment in the Himalayas, where metamorphic carbonates are exposed. The Irrawaddy and Salween have $^{87}Sr/^{86}Sr$ ratios similar to other major rivers draining the Eastern Himalaya–Tibetan mountain range, which provide over a quarter of the $^{87}Sr/^{86}Sr$ flux maintaining the high modern ocean $^{87}Sr/^{86}Sr$ ratio.

The discharge-weighted mean $^{87}Sr/^{86}Sr$ ratio for the Irrawaddy is 0.71024 ± 5 and the Salween is 0.71466 ± 6 close to their entry to the Andaman Sea. These rivers contribute a significant contribution to the global silicate weathering flux. The Irrawaddy and Salween carry about 3.3% of the global silicate weathering flux and 2.6% of the global riverine Sr flux. The Himalaya–Tibet catchment area covers just 4.8% of the total global area and the major rivers draining this area release 9.6% of global river discharge. The weathering fluxes from the rivers draining the Himalayan–Tibetan region are enhanced to deliver about 14% of the total Ca + Mg flux derived from silicates and 23% of the global riverine Sr flux. These fluxes are three to four times the output from the average continental area.

Supplementary data to this article can be found online at http://dx.doi.org/10.1016/j.chemgeo.2015.02.012.

Acknowledgements

We would like to thank the members of the Department of Meteorology & Hydrology, Myanmar, who collected the time-series samples in Myanmar, Sue Roddick who collected the three samples from the Mekong and Damien Calmels, the late Dr Fatima Khan who assisted with the analyses and Ruth Robinson who made her compilation of Gordon's discharge data on the Irrawaddy available to us. This paper has benefited from constructive comments by Jerome Gaillardet and an anonymous reviewer. Prof. Nay Htun and Mark Canning CMG (Ambassador at the British Embassy, Rangoon) facilitated this visit. The research was funded by the UK Natural Environmental Research Council grant NE/C513850/1.

References

Alford, D., 1992. Hydrological aspects of the Himalayan region. Occasional Paper. ICIMOD, Kathmandu, p. 68.

Allen, R., Carter, A., Najman, Y., Bandopadhyay, P., Chapman, H., Bickle, M., Garzanti, E., Vezzoli, G., Foster, G., 2008. New constraints on the sedimentation and uplift history of the Andaman-Nicobar accretionary prism, South Andaman Island. In: Draut, A., Clift, P.D., Scholl, D.W. (Eds.), Formation and Applications of the Sedimentary Record in Arc-Collision Zones. Geological Society of America, pp. 223–255.

Anderson, S.P., Dietrich, W.E., Montgomery, D.R., Torres, R., Loague, K., 1997. Concentration–discharge relationships in runoff from a steep, unchanneled catchment. Water Resour. Res. 33, 211–225.

Army Map Service (LUEN), C.o.E., 1955. U502, 1-AMS ed. 1:250,000, U.S. Army, Washington.

Bickle, M.J., 1996. Metamorphic decarbonation, silicate weathering and the long-term carbon cycle. Terra Nova 8, 270–276.

Bickle, M.J., Harris, N.B.W., Bunbury, J., Chapman, H.J., Fairchild, I.J., Ahmad, T., 2001. Controls on the 87Sr/86Sr of carbonates in the Garwal Himalaya, headwaters of the Ganges. J. Geol. 109, 737–753.

Bickle, M.J., Bunbury, J., Chapman, H.J., Harris, N.B., Fairchild, I.J., Ahmad, T., 2003. Fluxes of Sr into the headwaters of the Ganges. Geochim. Cosmochim. Acta 67, 2567–2584.

Bickle, M.J., Chapman, H.J., Bunbury, J., Harris, N.B.W., Fairchild, I.J., Ahmad, T., Pomiès, C., 2005. The relative contributions of silicate and carbonate rocks to riverine Sr fluxes in the headwaters of the Ganges. Geochem. Cosmochim. Acta 69, 2221–2240.

Bickle, M.J., Tipper, E., Galy, A., Chapman, H.J., Harris, N.W.B., 2015. On discrimination between carbonate and silicate inputs to Himalayan rivers. Am. J. Sci. 315, 120–166.
Caldeira, K., Arthur, M.A., Berner, R.A., Lasaga, A.C., 1993. Cooling in the Cenozoic: discussion of 'Tectonic forcing of late Cenozoic climate' by Raymo, M.E. and Ruddiman, W.F. Nature 361, 123–124.
Calmels, D., Galy, A., Hovius, N., Bickle, M., West, A.J., Chen, M.C., Chapman, H., 2011. Contribution of deep groundwater to the weathering budget in a rapidly eroding mountain belt, Taiwan. Earth Planet. Sci. Lett. 303, 48–58.
Chen, J., Wang, F., Xia, X., Zhang, L., 2002. Major element chemistry of the Changjiang (Yangtze River). Chem. Geol. 187, 231.
Chen, F.W., Wang, F., Meybeck, M., He, D., Xia, X., Zhang, L., 2005. Spatial and temporal analysis of water chemistry records (1958–2000) in the Huanghe (Yellow River) basin. Glob. Biogeochem. Cycles 19, GB3016 (24 pp.).
Clark, M.K., Schoenbohm, L.M., Royden, L.H., Whipple, K.X., Burchfiel, B.C., Zhang, X., Tang, W., Wang, E., Chen, L., 2004. Surface uplift, tectonics, and erosion of eastern Tibet from large-scale drainage patterns. Tectonics 23, TC1006 (20 pp.).
Daly, M.C., Cooper, M.A., Wilson, I., Smith, D.G., Hooper, B.G.D., 1991. Cenozoic plate tectonics and basin evolution in Indonesia. Mar. Pet. Geol. 8, 2–21.
Darbyshire, D.P.F., Swainbank, I.G., 1988. Geochronology of a selection of granites from Burma. NERC Isotope Geology Centre Report 88/006.
de Villiers, S., Greaves, M., Elderfield, H., 2002. An intensity ratio calibration method for the accurate determination of Mg/Ca and Sr/Ca of marine carbonates by ICP-AES. Geochem. Geophys. Geosyst. 3. http://dx.doi.org/10.1029/2001GC000169.
Dessert, C., Dupré, B., François, L., Schott, J., Gaillardet, J., Chakrapani, G., Bajpai, S., 2003. Erosion of Deccan Traps determined by river geochemistry: impact on the global climate and the 87Sr/86Sr ratio of seawater. Earth Planet. Sci. Lett. 188, 459–474.
Edmond, J.M., 1992. Himalayan tectonics, weathering processes, and the strontium isotope record in marine limestones. Science 258, 1594–1597.
English, N.B., Quade, J., DeCelles, P.G., Garzione, C., 2000. Geologic control of Sr and major element chemistry in Himalayan rivers, Nepal. Geochim. Cosmochim. Acta 64, 2549–2566.
Fontorbe, G., De La Rocha, C.L., Chapman, H.J., Bickle, M.J., 2013. The silicon isotopic composition of the Ganges and its tributaries. Earth Planet. Sci. Lett. 381, 21–30.
Gaillardet, J., Dupre, B., Louvat, P., Allegre, C.J., 1999. Global silicate weathering and CO_2 consumption rates deduced from the chemistry of large rivers. Chem. Geol. 159, 3–30.
Galy, A., France-Lanord, C., 1999. Weathering processes in the Ganges–Brahmaputra basin and the river alkalinity budget. Chem. Geol. 159, 31–60.
Galy, A., France-Lanord, C., Derry, L.A., 1999. The strontium isotopic budget of Himalayan Rivers in Nepal and Bangladesh. Geochim. Cosmochim. Acta 63, 1905–1925.
Gordon, R., 1879–1880. Report on the Irawadi River, Rangoon. p. 550.
Harris, N.B.W., Bickle, M.J., Chapman, H.J., Fairchild, I., Bunbury, J., 1998. The significance of Himalayan rivers for silicate weathering rates: evidence from the Bhoti Kosi tributary. Chem. Geol. 144, 205–220.
Jacobson, A.D., Blum, J.D., Walter, L.M., 2002. Reconciling the elemental and Sr isotope composition of Himalayan weathering fluxes: insights from the carbonate chemistry of stream waters. Geochim. Cosmochim. Acta 66, 3417–3429.
Krishnamurthy, R., Bhattacharya, S., 1991. Stable oxygen and hydrogen isotope ratios in shallow ground waters from India and a study of the role of evapotranspiration in the Indian monsoon. In: Taylor, H.P., O'Neil, J.R., Kaplan, R. (Eds.), Stable Isotope Geochemistry: A Tribute to Samuel Epstein. Geochem. Society, Special Publication, pp. 187–203.
Krishnaswami, S., Singh, S.K., 1998. Silicate and carbonate weathering in the drainage basins of the Ganga–Ghaghara–Indus head waters: contributions to major ion and Sr isotope geochemistry. Proc. Indian Acad. Sci. Earth Planet. Sci. 107, 283–291.
Krishnaswami, S., Trivedi, J.R., Sarin, M.M., Ramesh, R., Sharma, K.K., 1992. Strontium isotopes and rubidium in the Ganga–Brahmaputra river system: weathering in the Himalaya, fluxes to the bay of Bengal and contributions to the evolution of oceanic 87Sr/86Sr. Earth Planet. Sci. Lett. 109, 243–253.
Li, S., Lu, X.X., Bush, R.T., 2014. Chemical weathering and CO_2 consumption in the Lower Mekong River. Sci. Total Environ. 472, 162–177.
Maury, R.C., Pubellier, M., Rangin, C., Wulput, L., Cotten, J., Socquet, A., Hervé Bellon, H., Guillaud, J.-P., Htun, H.M., 2004. Quaternary calc-alkaline and alkaline volcanism in an hyper-oblique convergence setting, central Myanmar and western Yunnan. Bull. Soc. Géol. France 175, 461–472.
Meybeck, M., Carbonnel, J.P., 1975. Chemical transport by the Mekong river. Nature 255, 134–136.
Meybeck, M., Ragu, A., 1996. River discharges to the oceans, an assessment of suspended solids, major ions, and nutrients. Environment Information and Assessment Report. UNEP, Nairobi.
Michalopoulos, P., Aller, R.C., 1995. Rapid clay mineral formation in Amazon delta sediments: reverse weathering and oceanic elemental cycles. Science 270, 614–617.
Milliman, J.D., Meade, R.H., 1983. Worldwide delivery of river sediments to the oceans. J. Geol. 91, 1–19.
Mitchell, A.H.G., 1993. Cretaceous–Cenozoic tectonics events in the western Myanmar (Burma) Assam region. J. Geol. Soc. 150, 1089–1102.
Mitchell, A.H.G., Htay, Myint Thein, Htun, Kyaw Min, Win, Myint Naing, Oo, Thura, Hlaing, Tin, 2007. Rock relationships in the Mogok metamorphic belt, Tatkon to Mandalay, central Myanmar. J. Asian Earth Sci. 29, 891–910.
Mitchell, A., Chung, S.-L., Oo, T., Lin, T.-H., Hung, C.-H., 2012. Zircon U–Pb ages in Myanmar: magmatic-metamorphic events and the closure of a neo-Tethys ocean? J. Asian Earth Sci. 56, 1–23.
Moon, S., Huh, Y., Qin, J., van Pho, N., 2007. Chemical weathering in the Hong (Red) River basin: rates of silicate weathering and their controlling factors. Geochim. Cosmochim. Acta 71, 1411–1430.
Moon, S., Chamberlain, C.P., Hilley, G.P., 2014. New estimates of silicate weathering rates and their uncertainties in global rivers. Geochim. Cosmochim. Acta 134, 257–274.
Najman, Y., Johnson, C., White, N.M., Oliver, G., 2004. Evolution of the Himalayan foreland basin, NW India. Basin Res. 16, 1–24.
New, M., Lister, D., Hulme, M., Makin, I., 2002. A high-resolution data set of surface climate over global land areas. Clim. Res. 21, 1–25.
Palmer, M., Edmond, J.M., 1989. The strontium isotope budget of the modern ocean. Earth Planet. Sci. Lett. 92, 11–26.
Pandey, S.K., Singh, A.K., Hasnain, S.I., 1999. Weathering and geochemical processes controlling solute acquisition in Ganga headwater–Bhagirathi river, Garhwal Himalaya, India. Aquat. Geochem. 5, 357–379.
Peucker-Ehrenbrink, B., Miller, M.W., Asrsouze, T., Jeandel, C., 2010. Continental bedrock and riverine fluxes of strontium and neodymium isotopes to the oceans. Geochem. Geophys. Geosyst. 11 (3), Q03016. http://dx.doi.org/10.1029/2009GC002869 (22 pp).
Raymo, M.E., Ruddiman, W.F., 1992. Tectonic forcing of late Cenozoic climate. Nature 359, 117–122.
Raymo, M.E., Ruddiman, W.F., Froelich, P.N., 1988. Influence of late Cenozoic mountain building on ocean geochemical cycles. Geology 16, 649–653.
Richter, F.M., Rowley, D.B., DePaolo, D.J., 1992. Sr isotope evolution of seawater: the role of tectonics. Earth Planet. Sci. Lett. 109, 11–23.
Robinson, R.A.J., Bird, M.J., Oo, N.W., Hoey, T.B., Maung Aye, M., Higgitt, D.L., Lu, X.X., Sandar Aye, K., Swe, A., Tun, T., Lhaing Win, .S., 2007. The Irrawaddy river sediment flux to the Indian ocean: the original nineteenth-century data revisited. J. Geol. 115, 629–640.
Robinson, R.A.J., Brezina, C.A., Parrish, R.A., Horstwood, M.S.A., Win Oo, N., Bird, M.I., Thein, M., Walters, A.S.W., Oliver, G.J.H., Zaw, K., 2013. Large rivers and orogens: the evolution of the Yarlung Tsangpo–Irrawaddy system and the eastern Himalayan syntaxis. Gondwana Res. http://dx.doi.org/10.1016/j.gr.2013.07.002.
Sarin, M.M., Krishnaswami, S., Dilli, K., Somayajulu, B.L.K., Moore, W.S., 1989. Major ion chemistry of the Ganga–Brahmaputra river system: weathering processes and fluxes to the Bay of Bengal. Geochim. Cosmochim. Acta 53, 997–1009.
Searle, M.P., Noble, S.R., Cottle, J.M., Waters, D.J., Mitchell, A.H.G., Hlaing, T., Horstwood, M.S.A., 2007. Tectonic evolution of the Mogok metamorphic belt, Burma (Myanmar) constrained by U–Th–Pb dating of metamorphic and magmatic rocks. Tectonics 26, TC3014.
Singh, A.K., Hasnain, S.I., 1998. Major ion chemistry and weathering control in a high altitude basin: Alaknanda River, Garhwal Himalaya, India. Hydrol. Sci. J. 43, 825–843.
Singh, S.K., Sarin, M.M., France-Lanord, C., 2005. Chemical erosion in the eastern Himalaya: Major ion composition of the Brahmaputra and □13C of dissolved inorganic carbon. Geochim. Cosmochim. Acta 69, 3573–3588.
Stephenson, D., Marshall, T.R., 1984. The petrology and mineralogy of Mt Popa Volcano and the nature of the late-Cenozoic Burma Volcanic Arc. J. Geol. Soc. 141, 747–762.
Szulc, A.G., Najman, Y., Sinclair, H.D., Pringle, M., Bickle, M., Chapman, H., Garzanti, E., Ando, S., Huyghe, P., Mugnier, J.L., Ojha, T., DeCelles, P., 2006. Tectonic evolution of the Himalaya constrained by detrital Ar-40–Ar-39, Sm–Nd and petrographic data from the Siwalik foreland basin succession, SW Nepal. Basin Res. 18, 375–391.
Tipper, E.T., Bickle, M.J., Galy, A., West, A.J., Pomiès, C., Chapman, H.J., 2006. The short term climatic sensitivity of carbonate and silicate weathering fluxes: insight from seasonal variations in river chemistry. Geochim. Cosmochim. Acta 70, 2737–2754.
Tipper, E.T., Gaillardet, J., Galy, A., Louvat, P., Bickle, M.J., Capmas, F., 2010. Calcium isotope ratios in the world's largest rivers: a constraint on the maximum imbalance of oceanic calcium fluxes. Glob. Biogeochem. Cycles 24, 13.
Torres, M.A., West, A.J., Li, G., 2014. Sulphide oxidation and carbonate dissolution as a source of CO_2 over geological timescales. Nature 507, 346–349.
Turchyn, A.V., Tipper, E., Galy, A., Lo, J., Bickle, M.J., 2013. Isotope evidence for secondary sulfide precipitation along the Marsyandi River, Nepal, Himalayas. Earth Planet. Sci. Lett. 374, 36–46.
Wang, Z.-L., Zhang, J., Liu, C.-Q., 2007. Strontium isotopic compositions of dissolved and suspended loads from the main channel of the Yangtze River. Chemosphere 69, 1081–1088.
West, A.J., Bickle, M.J., Collins, R., Brasington, J., 2002. A small catchment perspective on Himalayan weathering fluxes. Geology 30, 355–358.
Zhang, S.-R., Lu, X.X., Higgitt, D.L., Chen, C.-T.A., Sun, H.-G., Han, J.-T., 2007. Water chemistry of the Zhujiang (Pearl River): natural processes and anthropogenic influences. J. Geophys. Res. 112, F01011.
Zhang, S.-R., Lu, X.X., Higgitt, D.L., Chen, C.-T.A., Han, J., Sun, H., 2008. Recent changes of water discharge and sediment load in the Zhujiang (Pearl River) Basin, China. Glob. Planet. Chang. 60, 365–380.
Zin, W.W., Nestmann, F., Ihringer, J., 2009. Flood forecasting using FGM model in Chindwin river basin. Malays. J. Civ. Eng. 21, 135–151.